

1-M98M411c.2
CPUB



Energy, Mines and
Resources Canada

Énergie, Mines et
Ressources Canada

CANMET

Canada Centre for
Mineral and Energy
Technology

Centre canadien de la
technologie des
minéraux et de l'énergie

**Mining
Research
Laboratories**

**Laboratoires
de recherche
minière**

STABILITY ASSESSMENT OF S-L-102-19/S-102-21 SILL
PILLARS AND ADJACENT STOPES OF THE NIOBEC MINE,
CHICOUTIMI, QUEBEC – PART IV

Y.S. Yu, A.S. Wong and N.A. Toews

MRL 88-101(TR)
C.2

Canada

This document was produced
by scanning the original publication.

Ce document est le produit d'une
numérisation par balayage
de la publication originale.

MRL 88-101(TR)c.2

MRL 88-101(TR)c.2



1-798771c.2
CPQB

STABILITY ASSESSMENT OF S-L-102-19/S-102-21 SILL
PILLARS AND ADJACENT STOPES OF THE NIOBEC MINE,
CHICOUTIMI, QUEBEC - PART IV 1-798771c.2 CPQB

Y.S. Yu, A.S. Wong and N.A. Toews

MRL 88-101(TR)
C.2



c.2
CPQB

STABILITY ASSESSMENT OF S-L-102-19/S-102-21 SILL PILLARS AND
ADJACENT STOPES OF THE NIOBEC MINE, CHICOUTIMI, QUEBEC - PART IV

by
Y.S. Yu*, A.S. Wong**, and N.A. Toews*

ABSTRACT

A series of co-operative research studies on mine stability has been carried out with the participation of the Niobec Mine, Chicoutimi, Quebec. Part IV, in part, involves a stability evaluation of S-L-102-19 and S-102-21 sill pillars and adjacent areas under measured mine stress conditions. Analytic studies were also carried out to evaluate the effect of extraction of the support pillars at the upper level on the overall stability of the mine structure. Three-dimensional finite element techniques were used in these studies.

It was established that under actual field stress conditions the effect of mining C-102-19 and C-102-21 stopes (lower mining blocks) on ground stability conditions around stopes at the upper mining blocks would be nominal. In addition, the recovery of support pillars at the upper levels did not produce large compressive stresses which could jeopardize the integrity of the mine structure. However, localized tensile failure may occur around the stopes.

Based on the use of Drucker/Prager yield criterion, Hoek and Brown's empirical failure criterion, and assumptions concerning in situ rock properties, analytic studies indicated no potential failure zones. However, tensile stresses did occur in stope walls and pillars reaching a maximum value of 1.77 MPa. Therefore, localized tensile failure was established as a possibility if joints were unfavorably oriented with respect to tensile stresses.

Key words: Niobec Mine, stability, three-dimensional stresses, factor of safety, finite element,

* Research Scientists, ** Physical Scientist, Mining Research Laboratories, CANMET, Energy, Mines and Resources Canada, Ottawa.

*EVALUATION DES PILIERS DE SOLE S-L-102-19/S-102-21 ET DES CHANTIERS
ADJACENTS DE LA MINE NIOBEC, CHICOUTIMI (QUEBEC) – PARTIE IV*

par
Y.S. Yu*, A.S. Wong** et N.A. Toews*

RÉSUMÉ

Une série de recherches conjointes sur la stabilité des mines a été effectuée avec la participation de la mine Niobec de Chicoutimi au Québec. La partie IV porte en partie sur une évaluation de la stabilité des piliers de sole S-L-102-19 et S-102-21 et des zones adjacentes dans des conditions de contraintes minières mesurées. Des études analytiques ont aussi été menées pour évaluer l'effet de l'extraction des piliers de soutènement au niveau supérieur sur la stabilité globale de la structure d'une mine. Des techniques d'analyse tridimensionnelle par éléments finis ont été utilisées dans ces études.

Il a été établi que, sous l'action de contraintes réelles sur le terrain, l'exploitation des chantiers C-102-19 et C-102-21 (blocs d'exploitation inférieurs) aurait un effet nominal sur les conditions de stabilité du terrain autour des chantiers situés dans des blocs supérieurs. En outre, la récupération des piliers de soutènement des niveaux supérieurs n'a pas donné lieu à d'importantes contraintes de compression qui pourraient menacer l'intégrité de la structure de la mine. Toutefois, des ruptures de traction localisées peuvent se produire autour des chantiers.

Basé sur la limite d'élasticité de Drucker/Prager, le critère de rupture empirique de Hoek et Brown et des hypothèses sur les propriétés de la roche *in situ*, les études analytiques n'ont révélé aucune zone de rupture potentielle. Des contraintes de traction ont toutefois été observées dans les fronts d'abattage et les piliers, atteignant un maximum de 1,77 MPa. Il a donc été établi que des ruptures de traction localisées étaient possibles lorsque les joints n'étaient pas favorablement orientés par rapport aux contraintes de traction.

Mots clés: mine Niobec, stabilité, contraintes tridimensionnelles, facteur de sécurité, élément fini

*Chercheur scientifiques, ** Physicien, Laboratoires de recherche minière, CANMET, Energie, Mines et Ressources Canada, Ottawa.

CONTENTS

	<u>page</u>
ABSTRACT	i
RÉSUMÉ	ii
1.0 INTRODUCTION	1
2.0 THE NIOBEC MINE	1
2.1 3-D Niobec Mine Model	4
2.2 Material Properties of the Mine Rocks	9
2.3 Field Stresses	10
3.0 RESULTS	10
3.1 Stress Distribution	10
3.2 Potential Failure Areas	19
3.2.1 Drucker/Prager Yield Criterion	20
3.2.2 Hoek and Brown's Empirical Failure Criterion	20
4.0 CONCLUSIONS AND RECOMMENDATIONS	21
5.0 ACKNOWLEDGEMENTS	30
6.0 REFERENCES	30

FIGURES

1. A plan view of the Niobec Mine at Level 300	2
2. A longitudinal section at 150 + 50N	3
3(a). An isometric view of the 3-D Niobec Mine model	5
3(b). The finite element discretization for section $x = 106.68$ m	6
3(c). The finite element discretization for section $x = 99.09$ m	7
3(d). The finite element discretization for section $x = 0.0$ m	8
4. Major principal stress contour, for section $x = 102.87$ m	11
5. Major principal stress contour, for section $x = 95.25$ m	12
6. Major principal stress contour, for section $x = 88.39$ m	13
7. Major principal stress contour, for section $x = 82.29$ m	14
8. Minor principal stress contour, for section $x = 102.87$ m	15
9. Minor principal stress contour, for section $x = 95.25$ m	16
10. Minor principal stress contour, for section $x = 88.39$ m	17
11. Minor principal stress contour, for section $x = 82.29$ m	18

	<u>page</u>
12. Local factor of safety contour plot ($C=4$ MPa, $\phi = 40^\circ$) for section $x = 102.87\text{m}$	22
13. Local factor of safety contour plot ($C = 4$ MPa, $\phi = 40^\circ$) for section $x = 95.27\text{m}$	23
14. Local factor of safety contour plot ($C = 4$ MPa, $\phi = 40^\circ$) for section $x = 88.39\text{m}$	24
15. Local factor of safety contour plot ($C = 4$ MPa, $\phi = 40^\circ$) for section $x = 82.29\text{m}$	25
16. Strength/stress ratio - Hoek & Brown's empirical failure criterion ($m = 3.30$, $s = 0.1111$) for section $x = 102.87\text{m}$	26
17. Strength/stress ratio - Hoek & Brown's empirical failure criterion ($m = 3.30$, $s = 0.1111$) for section $x = 95.25\text{m}$	27
18. Strength/stress ratio - Hoek & Brown's empirical failure criterion ($m = 3.30$, $s = 0.1111$) for section $x = 88.39\text{m}$	28
19. Strength/stress ratio - Hoek & Brown's empirical failure criterion ($m = 3.30$, $s = 0.1111$) for section $x = 82.29\text{m}$	29

TABLE

1. Material properties of geological formations used for modelling study	9
--	---

1.0 INTRODUCTION

A cooperative study program on mine stability evaluation was initiated in 1985 involving Niobec Mine, Centre de Recherches Minérales, Quebec, and the CANMET's Mining Research Laboratories (MRL). The program was structured to meet both the ground control information requirements of Niobec Mines Ltd. and the broader ground control interests of its two partners. The objectives of the program are indicated below:

- (a) to contribute to the development of a geomechanical data-base on the physical and mechanical properties of mine rocks;
- (b) to determine the field stresses at the mine, and to design and test instruments to monitor stress changes as mining progresses;
- (c) to assess the regional and local stability of the mine structure by means of numerical simulation; and
- (d) to provide detailed study results and interpretations which may be considered for incorporation by mine engineering staff in making mine design and ground control decisions.

The Centre de Recherches Minérales assumed responsibility for carrying out tasks essential to achieving objective (a). The Mining Research Laboratories assumed responsibility for carrying out tasks essential to achieving objectives (b) through (d). In this regard, MRL carried out, in 1986, in situ stress determinations to provide input data on far field stresses for use in numerical analysis studies [1]. As well, mining induced stress changes were monitored in T213-13 pillar and in the vicinity of C-203-15 stope on the 850 level. MRL strain rings were used for this purpose.

The present report describes Part IV of a series of studies on numerical modelling concerning the structural stability assessment of the Niobec Mine. In this study, the stability of S-L-102-19 and S-102-21 sill pillars were analysed using three dimensional finite element techniques. In addition, the effect of mining stope C-102-21 at the lower mining block and removal of all support pillars on the upper block on the overall stope/pillar stability were also evaluated using the stresses determined from the 3D finite element analysis and based on both Drucker/Prager and Hoek & Brown's empirical failure criteria.

2.0 NIOBEC MINE

The layout of Niobec Mine and the general geological conditions encountered in the mine have been described in previous reports [2,3,4]. Figures 1 and 2 show

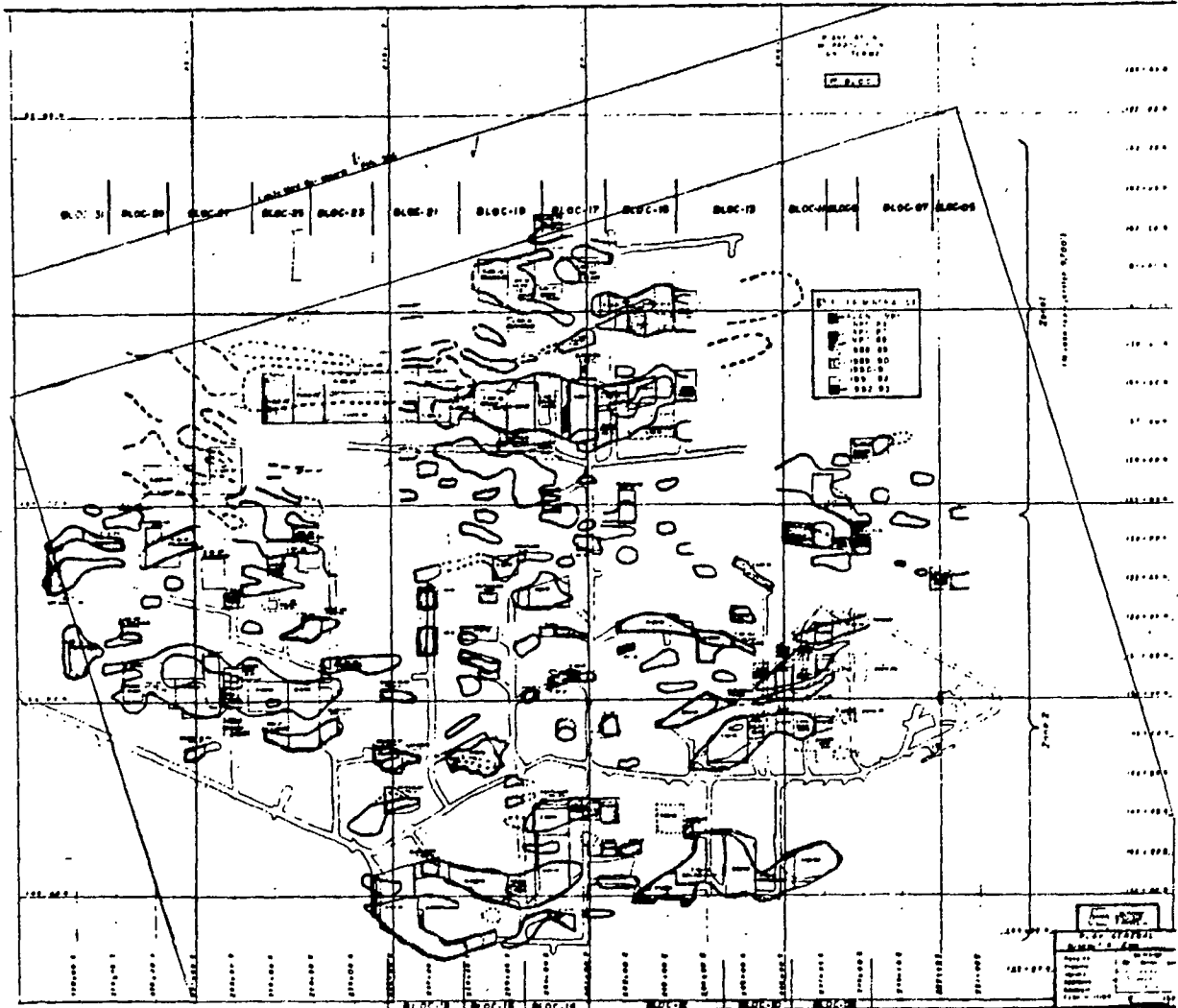


Fig. 1 A Plan View of the Niobec Mine at Level 300

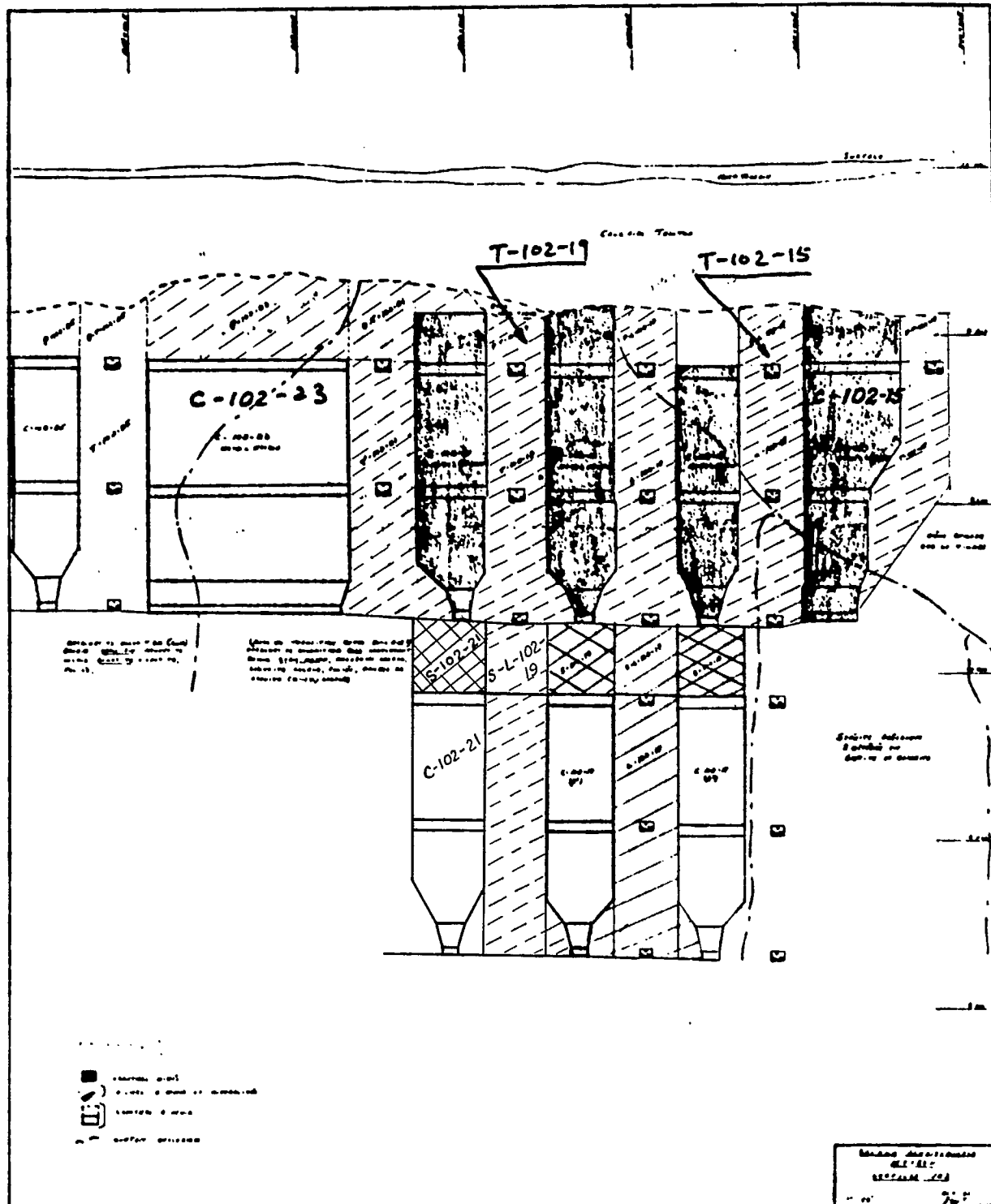


Fig. 2 A Longitudinal Section 157 + 50N of Niobec Mine

a plan view of the mine at the upper block and a longitudinal section of the mine (157+50N), respectively. Stopes C-102-21, C-102-19, C-102-17, C-102-15 have been completed mined. Stope C-102-23 at the upper block is currently under development with a planned stope span of 73m (240 ft) and width 30m. No instability has been observed.

Stability evaluation studies of C-102-23 stope under idealized loading conditions were previously completed [2,3,4,5]. The studies indicate that stope C-102-23 could be mined without major stability problems. However, tensile stresses could cause localized failure in the stope walls and pillars if joints are unfavorably oriented in relation to tensile stresses. Following completion of mining C-102-23 stope, the mine plans to recover of all pillars on the upper level and also mine additional stopes below the sill pillar C-102-21 (lower block). When all the upper block support pillars are extracted the stope span will stand at approximately 274m.

The present study was directed at evaluating the stability of sill pillars S-L-102-19 and S-102-21 induced by mining the stopes C-102-19 and C-102-21 (lower block); in addition, the impact of extracting all support pillars on the upper block on the overall stope/pillar stability at the Niobec Mine was examined.

2.1 3-D Niobec Mine Model

To evaluate the stability of sill pillars S-L-102-19 and S-102-21, a new 3-D mine model was constructed including stopes C-102-19 and C-102-21 located at the lower level. To simplify mine geometry for modelling purposes, the mine model was constructed with openings symmetric around the centre plane of pillar T-102-19. As a result, only one quarter of the total structure had to be modelled. However, this did result in including in the model a mirror image of stope C-102-23 not shown in Fig. 2. Its inclusion, however, was justified on the basis that the resulting model would result in analytic studies providing a conservative estimate of opening stabilities.

An isometric view of the finite element model used in the study is shown in Fig. 3(a). It represents only one quarter of the mine 'block' being simulated. Three typical model cross sections with their finite element discretization are shown in Fig. 3(b) to 3(d). The model was constructed with more refined discretization in the area of the sill pillar and the stopes below the sill pillar because of the particular study interest in their stability.

All stopes and pillars on the upper level, and stopes C-102-21 and C-102-19 which is a mirror image of stope C-102-21 below the sill pillar were all assumed to be mined.

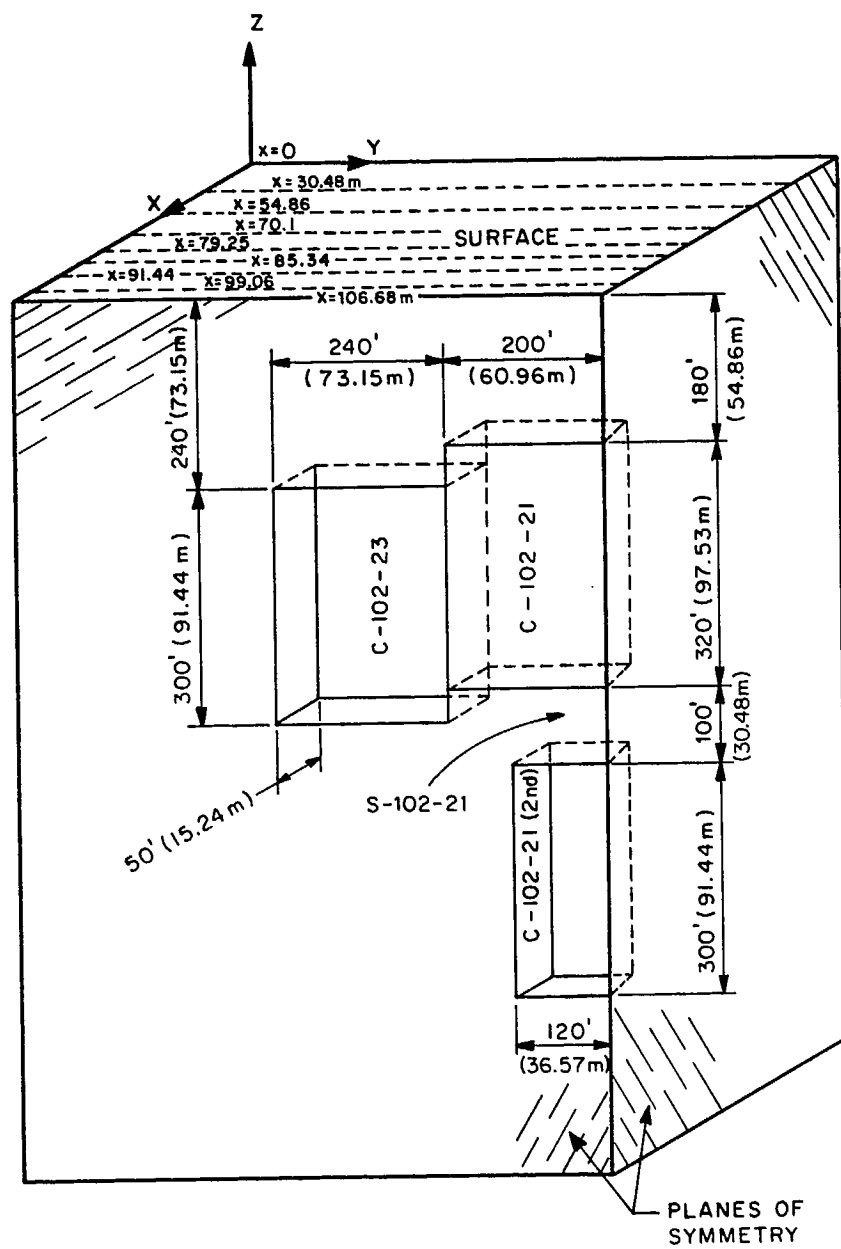
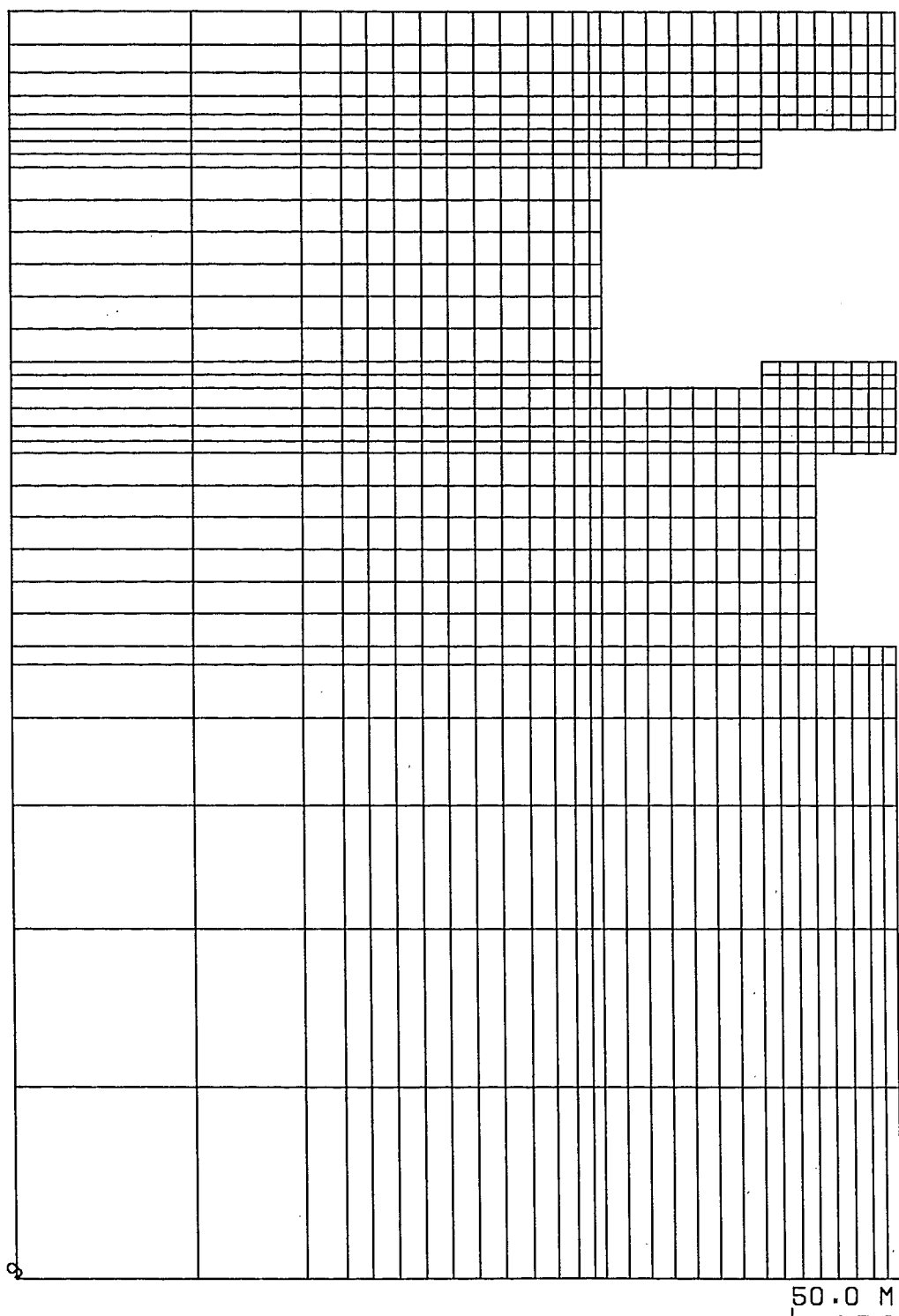


Fig. 3(a) An Isometric View of the 3-D Niobec Mine Model



SECTION = 9

Fig. 3(b) The Finite Element Discretization for Section $x = 106.68$ m.

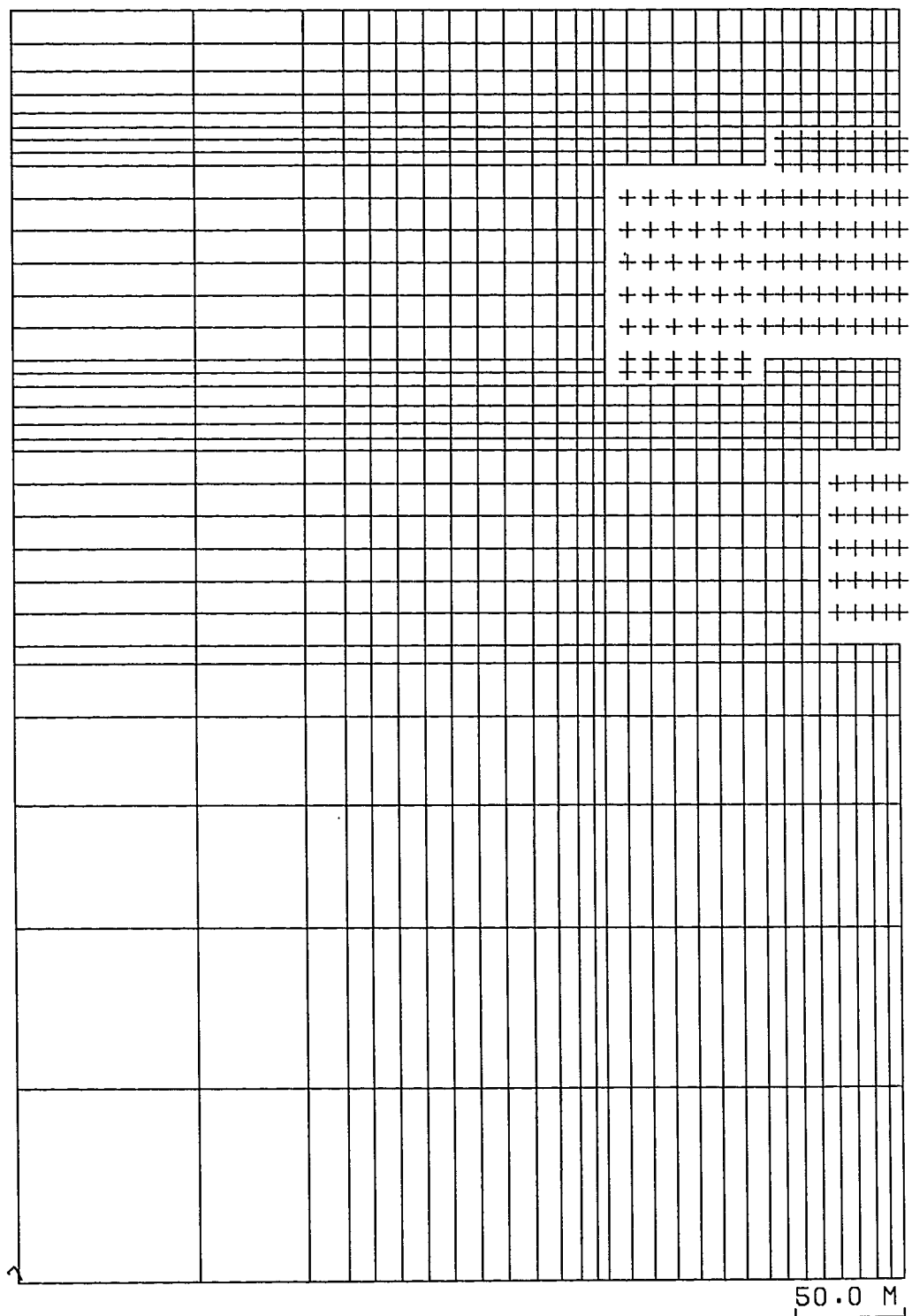


Fig. 3(c) The Finite Element Discretization for Section $x = 99.09$ m.

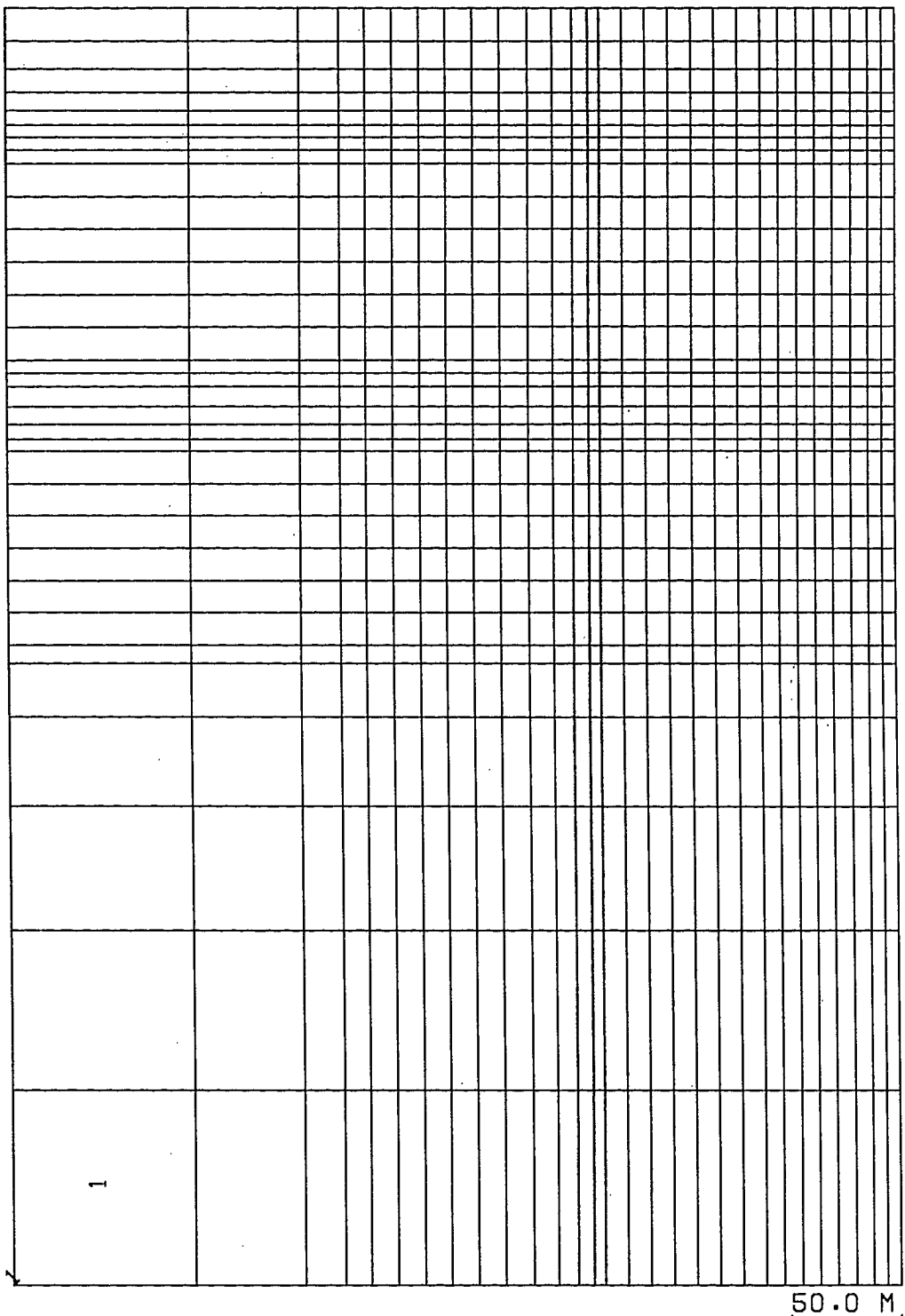


Fig. 3(d) The Finite Element Discretization for Section $x = 0.0$ m.

The computer model and the assumptions underlying its use in this study are the same as those used in previous studies. A basic eight-node brick element with three degrees of freedom at each node is used in the model. The model performs static, linear elastic analysis. Material properties are assumed to be isotropic. The model is capable of handling gravitational and distributed surface loads. Initial residual stresses, if known, can also be taken into consideration.

2.2 Material Properties of the Mine Rocks

The modulus of deformation, uniaxial compressive, and tensile strengths of both carbonatite and limestone capping the carbonatite formations were determined in laboratory tests [6,7]. A summary of the mechanical properties for the formations used in the study is given in Table 1.

Table 1 - Material Properties of the Geological Formations used in Modelling Study

Item	Limestone		Carbonatite (altered)		Carbonatite (intact)	
	Laboratory	Estimated*	Laboratory	Estimated*	Laboratory	Estimated*
Modulus of Deformation (MPa)	36,000	30,000	56,400	40,000	64,000	40,000
Poisson's Ratio	0.21	0.25	0.25	0.25	0.29	0.25
Uniaxial Compressive Strength (MPa)	92	45	86	45	128	45
Uniaxial Tensile Strength (MPa)	5.8	3.0	10.3	3.0	16.8	3.0
Cohesion (MPa)	10	2 - 4	17	2 - 4	25	2 - 4
Angle of Internal Friction (degrees)	36	40	50	40	51	40
Empirical Constant m	9.30	3.30	4.8	3.30	4.8	3.30
Empirical Constant s	0.04	0.1111	0.014	0.1111	0.014	0.1111
RQD's (%)	90		90		95	
* Used for modelling study;						

2.3 Field Stresses

In situ stress determinations were carried out in Niobec Mine at sites located at 270m and 320m in depth (levels 800 and 1000 respectively) [1].

In the Canadian Shield, it is known that horizontal stress is greater than vertical stress. Based on the limited stress data developed for the Niobec Mine, the following far field stress conditions were established.

$$\sigma_z = \gamma Z$$

$$\sigma_x = 1.5\sigma_z$$

$$\sigma_y = 2.0\sigma_z$$

where

σ_z = the vertical stress at depth Z ;

σ_x = the horizontal stress in the EW direction;

σ_y = the horizontal stress in the NS direction;

γ = the unit weight of rock material; and

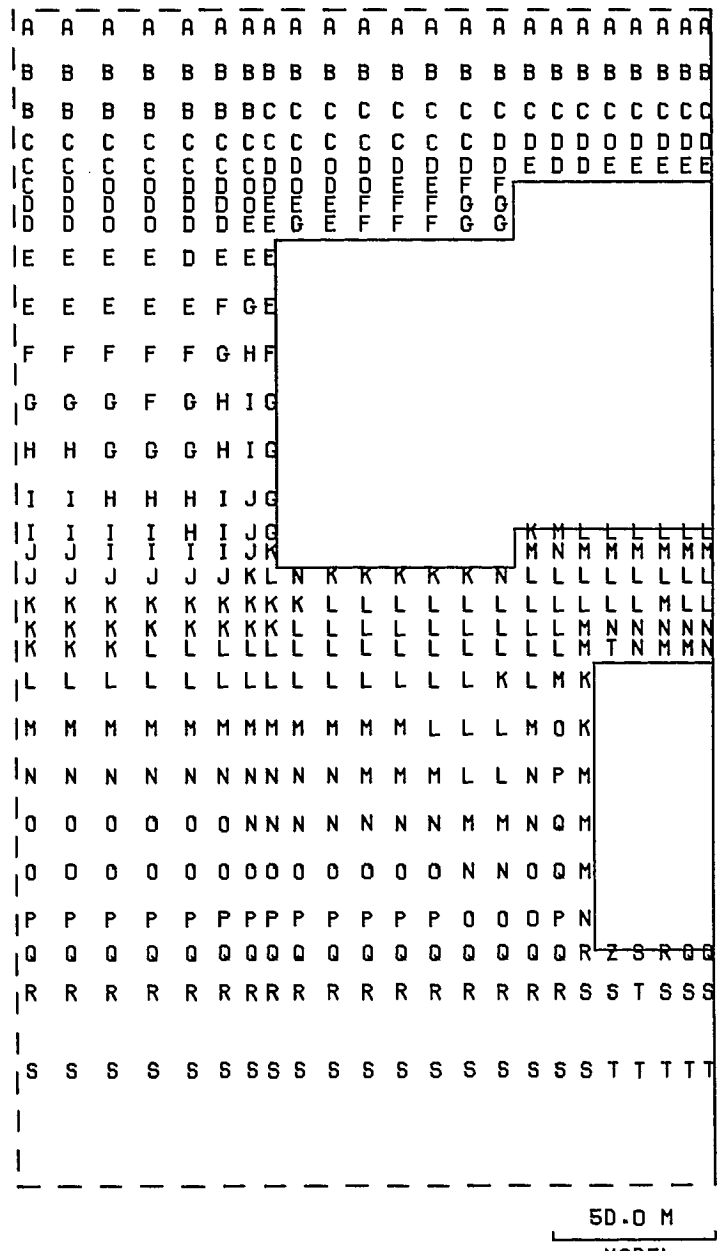
ν = Poisson's ratio.

This far field stresses were used to evaluate the stability of C-102-23 stope in Part II and Part III of the Niobec Mine stope stability assessment [3,4,5]. The same loading conditions were used in the present study.

3.0 RESULTS

3.1 Stress Distribution

Figures 4, 5, 6, and 7 show, respectively, the principal stress contours for sections $x = 102.87\text{m}$, 95.25m , 88.39m , and 82.29m . Stresses shown in Fig. 4 represent the average stresses in the central section ($x = 102.87\text{m}$) of the stope. Sections $x = 88.39\text{m}$ and 82.29m are located at about 3m and 9m, respectively, into the stope walls (hangingwall or footwall). All stresses are calculated at the centroid of each element which is located at the middle plane of each 'slice'. The minor principal stress contours for the same sections are shown in Fig. 8, 9, 10, and 11. Tensile stresses are developed in the floor, roof and wall of the large opening (stopes C-102-23, C-102-21 and C-102-19, and pillars T-102-21 and T-102-19) of the upper block, as shown in Fig. 8. Tensile zones penetrate into the large opening walls in the N-S direction approximately 9m as shown in Figs. 10 and 11.

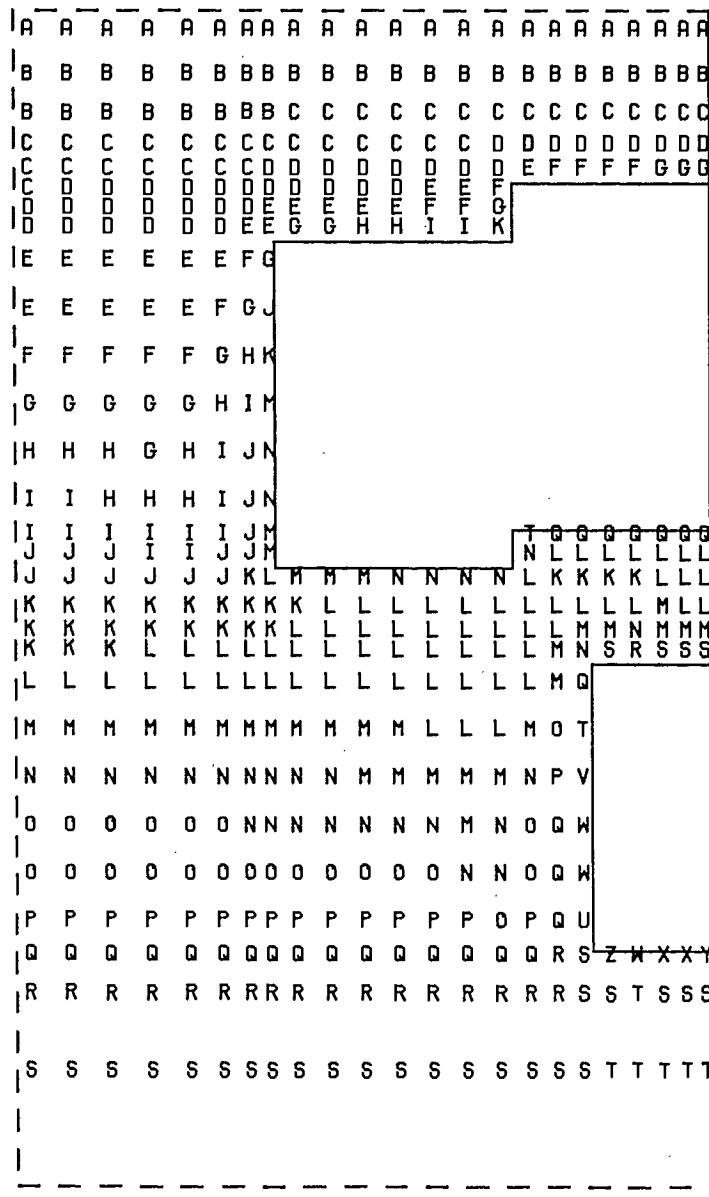


LEGEND

SYMBOL	RANGE
-	LESS 0.0
A	0.0 - 1.00
B	1.00 - 2.00
C	2.00 - 3.00
D	3.00 - 4.00
E	4.00 - 5.00
F	5.00 - 6.00
G	6.00 - 7.00
H	7.00 - 8.00
I	8.00 - 9.00
J	9.00 - 1.00E1
K	1.00E1 - 1.10E1
L	1.10E1 - 1.20E1
M	1.20E1 - 1.30E1
N	1.30E1 - 1.40E1
O	1.40E1 - 1.50E1
P	1.50E1 - 1.60E1
Q	1.60E1 - 1.70E1
R	1.70E1 - 1.80E1
S	1.80E1 - 1.90E1
T	1.90E1 - 2.00E1
U	2.00E1 - 2.10E1
V	2.10E1 - 2.20E1
W	2.20E1 - 2.30E1
X	2.30E1 - 2.40E1
Y	2.40E1 - 2.50E1
Z	2.50E1 - 2.60E1
+	GREATER OR EQUAL 2.60E1

MAXIMUM DATA VALUE 2.59E1
 MINIMUM DATA VALUE 3.62E-1
 STRESSES IN MPA

Fig. 4 Major principal stress contour plot for section x = 102.87 m.

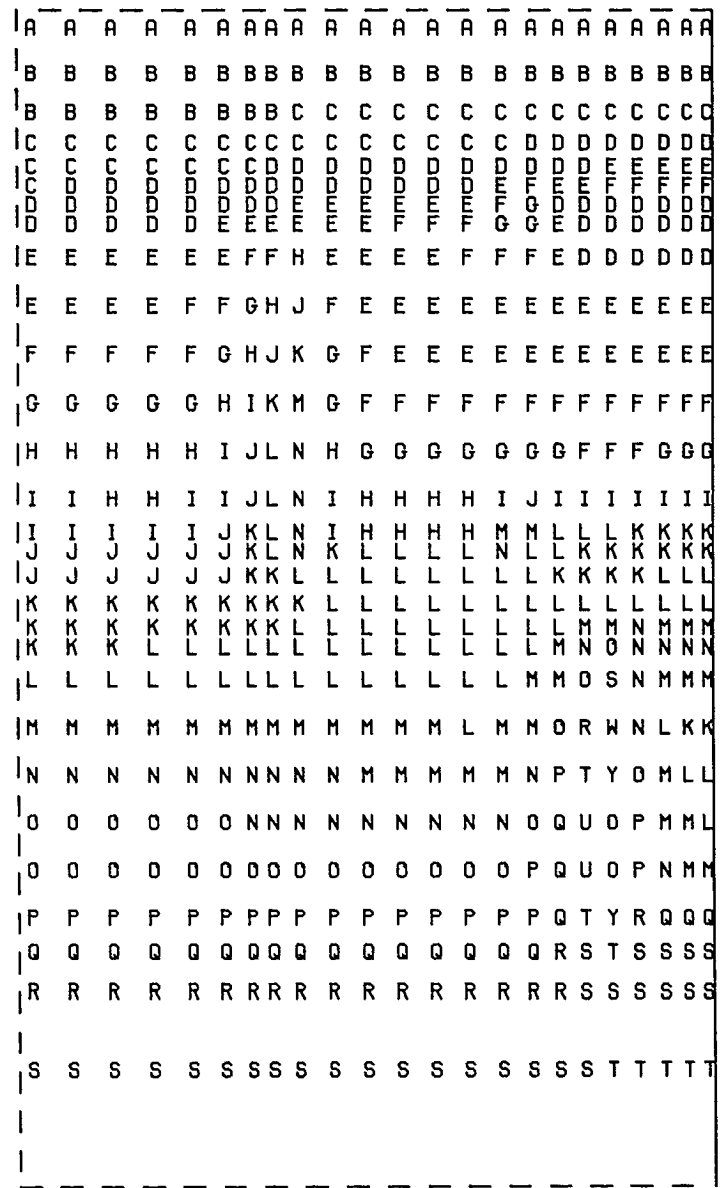


MAJOR PRINCIPAL STRESS CONTOURS X=95.25 M

SYMBOL	RANGE
-	LESS 0.0
A	0.0 - 1.00
B	1.00 - 2.00
C	2.00 - 3.00
D	3.00 - 4.00
E	4.00 - 5.00
F	5.00 - 6.00
G	6.00 - 7.00
H	7.00 - 8.00
I	8.00 - 9.00
J	9.00 - 1.00E1
K	1.00E1 - 1.10E1
L	1.10E1 - 1.20E1
M	1.20E1 - 1.30E1
N	1.30E1 - 1.40E1
O	1.40E1 - 1.50E1
P	1.50E1 - 1.60E1
Q	1.60E1 - 1.70E1
R	1.70E1 - 1.80E1
S	1.80E1 - 1.90E1
T	1.90E1 - 2.00E1
U	2.00E1 - 2.10E1
V	2.10E1 - 2.20E1
W	2.20E1 - 2.30E1
X	2.30E1 - 2.40E1
Y	2.40E1 - 2.50E1
Z	2.50E1 - 2.60E1
+	GREATER OR EQUAL 2.60E1

MAXIMUM DATA VALUE 2.50E1
MINIMUM DATA VALUE 3.62E-1
STRESSES IN MPa

Fig. 5 Major principal stress contour plot for section x = 95.25 m.



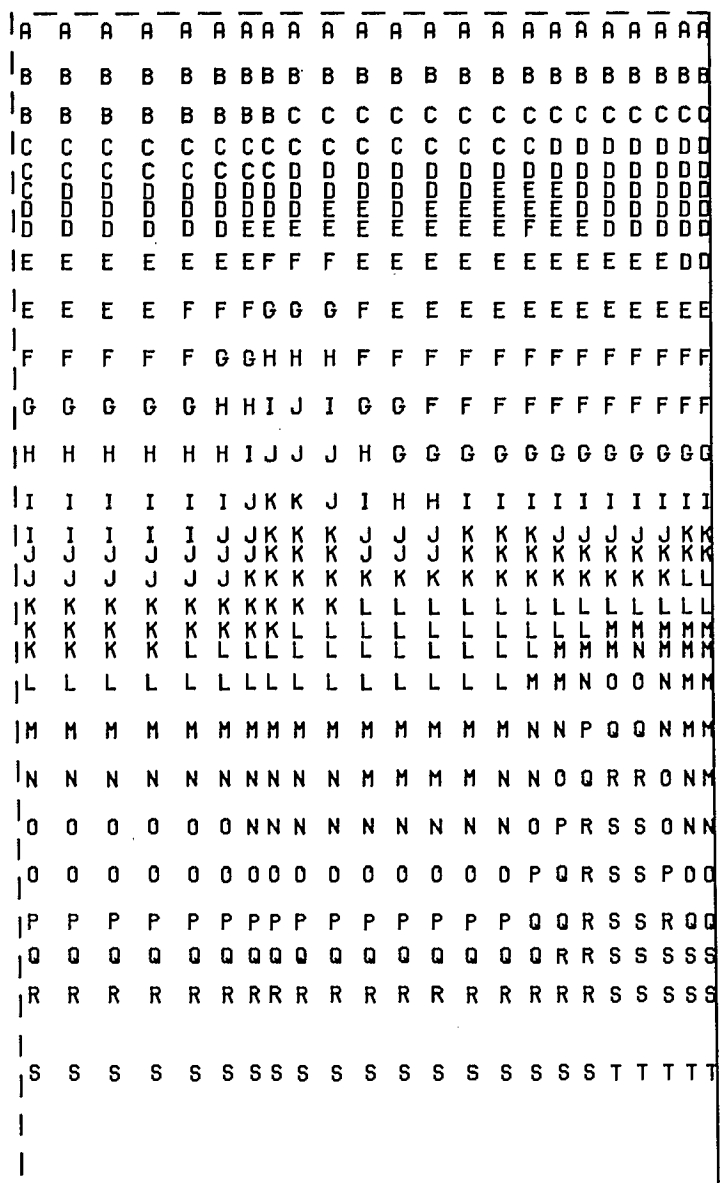
LEGEND

SYMBOL	RANGE
-	LESS 0.0
A	0.0 - 1.00
B	1.00 - 2.00
C	2.00 - 3.00
D	3.00 - 4.00
E	4.00 - 5.00
F	5.00 - 6.00
G	6.00 - 7.00
H	7.00 - 8.00
I	8.00 - 9.00
J	9.00 - 1.00E1
K	1.00E1 - 1.10E1
L	1.10E1 - 1.20E1
M	1.20E1 - 1.30E1
N	1.30E1 - 1.40E1
O	1.40E1 - 1.50E1
P	1.50E1 - 1.60E1
Q	1.60E1 - 1.70E1
R	1.70E1 - 1.80E1
S	1.80E1 - 1.90E1
T	1.90E1 - 2.00E1
U	2.00E1 - 2.10E1
V	2.10E1 - 2.20E1
W	2.20E1 - 2.30E1
X	2.30E1 - 2.40E1
Y	2.40E1 - 2.50E1
Z	2.50E1 - 2.60E1
O	2.60E1 - 2.70E1
+	GREATER OR EQUAL 2.70E1

MAXIMUM DATA VALUE 2.64E1
MINIMUM DATA VALUE 3.62E-1
STRESSES IN MPa

MAJOR PRINCIPAL STRESS CONTOURS X=88.39 M

Fig. 6 Major principal stress contour plot for section x = 88.39 m.



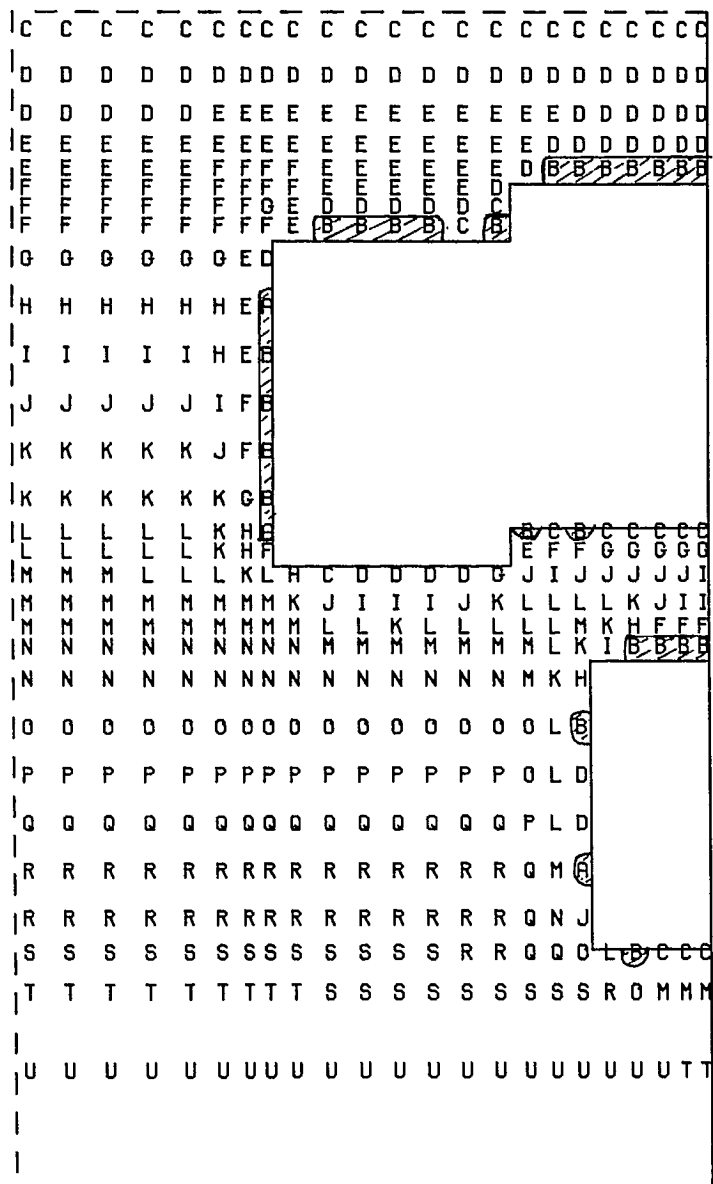
MAJOR PRINCIPAL STRESS CONTOURS X=82.29 M

LEGEND

SYMBOL	RANGE
-	LESS 0.0
A	0.0 - 1.00
B	1.00 - 2.00
C	2.00 - 3.00
D	3.00 - 4.00
E	4.00 - 5.00
F	5.00 - 6.00
G	6.00 - 7.00
H	7.00 - 8.00
I	8.00 - 9.00
J	9.00 - 1.00E1
K	1.00E1 - 1.10E1
L	1.10E1 - 1.20E1
M	1.20E1 - 1.30E1
N	1.30E1 - 1.40E1
O	1.40E1 - 1.50E1
P	1.50E1 - 1.60E1
Q	1.60E1 - 1.70E1
R	1.70E1 - 1.80E1
S	1.80E1 - 1.90E1
T	1.90E1 - 2.00E1
+	GREATER OR EQUAL 2.00E1

MAXIMUM DATA VALUE 1.93E1
MINIMUM DATA VALUE 3.61E-1
STRESSES IN MPa

Fig. 7 Major principal stress contour plot for section x = 82.29 m.

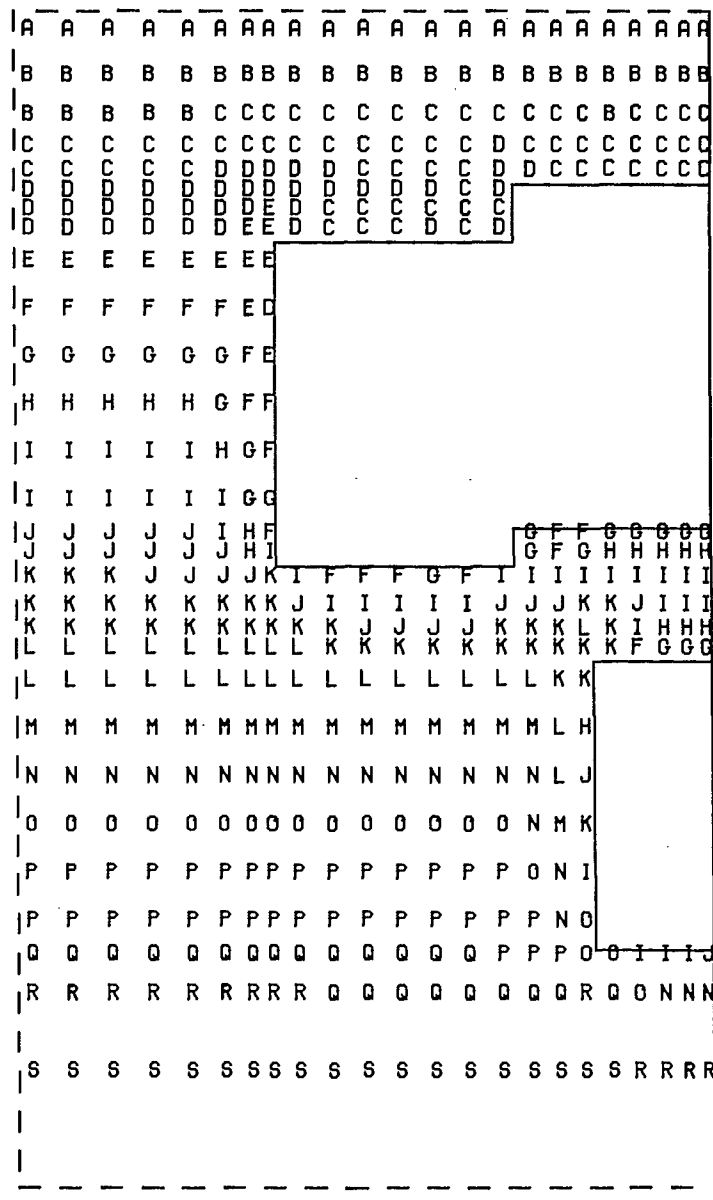


LEGEND

SYMBOL	RANGE
-	LESS -1.00
A	-1.00 - -5.00E-1
B	-5.00E-1 - 0.0
C	0.0 - 5.00E-1
D	5.00E-1 - 1.00
E	1.00 - 1.50
F	1.50 - 2.00
G	2.00 - 2.50
H	2.50 - 3.00
I	3.00 - 3.50
J	3.50 - 4.00
K	4.00 - 4.50
L	4.50 - 5.00
M	5.00 - 5.50
N	5.50 - 6.00
O	6.00 - 6.50
P	6.50 - 7.00
Q	7.00 - 7.50
R	7.50 - 8.00
S	8.00 - 8.50
T	8.50 - 9.00
U	9.00 - 9.50
+	GREATER OR EQUAL 9.50

MAXIMUM DATA VALUE 9.20
MINIMUM DATA VALUE -6.12E-1
STRESSES IN MPa

Fig. 8 Minor principal stress contour plot for section x = 102.87 m.

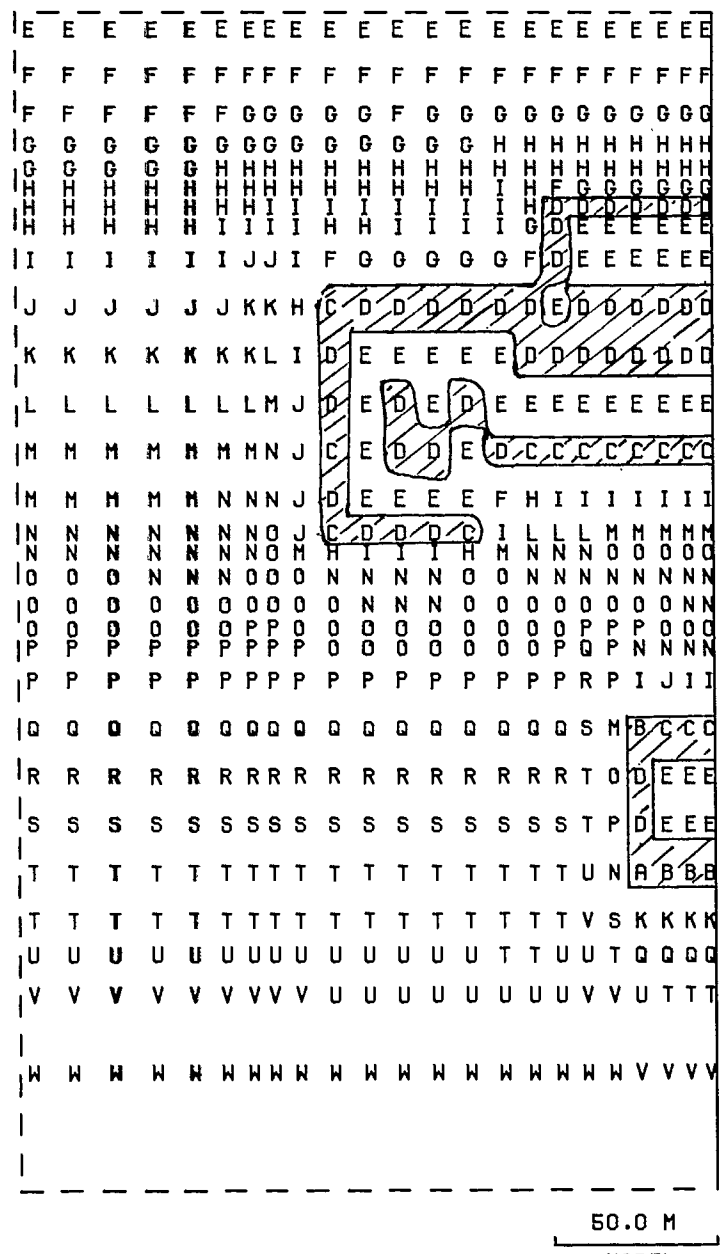


LEGEND

SYMBOL	RANGE
-	LESS 0.0
A	0.0 - 5.00E-1
B	5.00E-1 - 1.00
C	1.00 - 1.50
D	1.50 - 2.00
E	2.00 - 2.50
F	2.50 - 3.00
G	3.00 - 3.50
H	3.50 - 4.00
I	4.00 - 4.50
J	4.50 - 5.00
K	5.00 - 5.50
L	5.50 - 6.00
M	6.00 - 6.50
N	6.50 - 7.00
O	7.00 - 7.50
P	7.50 - 8.00
Q	8.00 - 8.50
R	8.50 - 9.00
S	9.00 - 9.50
+	GREATER OR EQUAL 9.50

MAXIMUM DATA VALUE 9.20
MINIMUM DATA VALUE 1.66E-1
STRESSES IN MPa

Fig. 9 Minor principal stress contour plot for section x = 95.25 m.

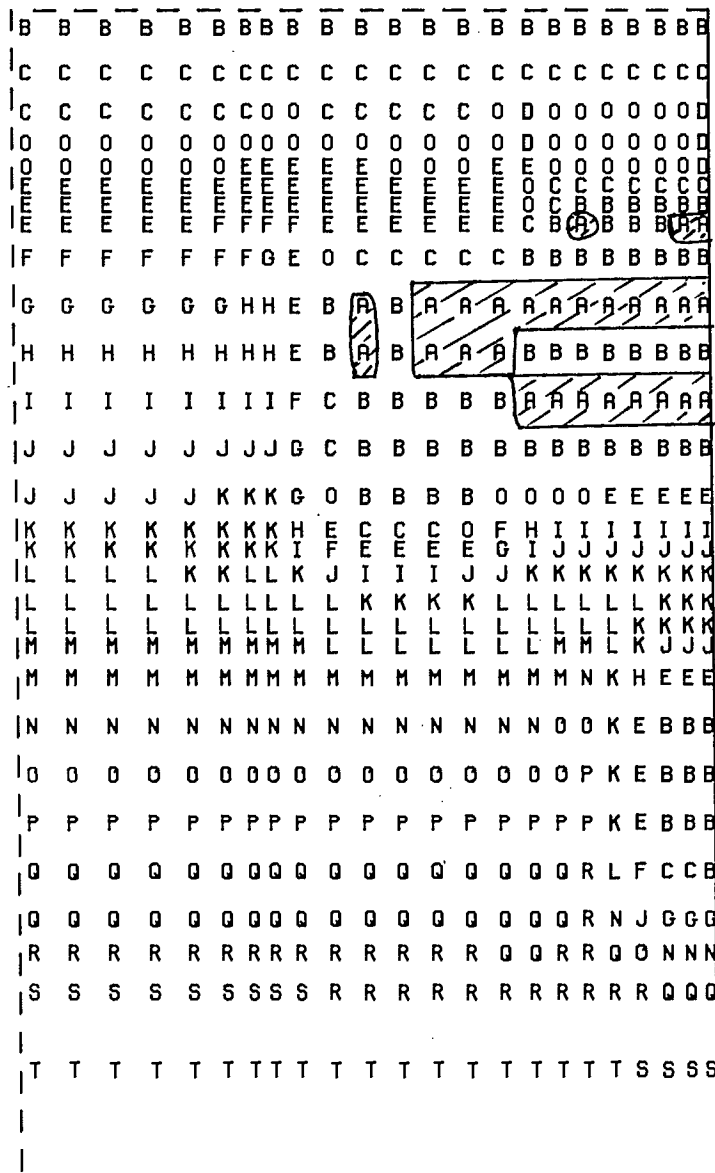


LEGEND

SYMBOL	RANGE
-	LESS -2.00
A	-2.00 - -1.50
B	-1.50 - -1.00
C	-1.00 - -5.00E-1
D	-5.00E-1 - 0.0
E	0.0 - 5.00E-1
F	5.00E-1 - 1.00
G	1.00 - 1.50
H	1.50 - 2.00
I	2.00 - 2.50
J	2.50 - 3.00
K	3.00 - 3.50
L	3.50 - 4.00
M	4.00 - 4.50
N	4.50 - 5.00
O	5.00 - 5.50
P	5.50 - 6.00
Q	6.00 - 6.50
R	6.50 - 7.00
S	7.00 - 7.50
T	7.50 - 8.00
U	8.00 - 8.50
V	8.50 - 9.00
W	9.00 - 9.50
+	GREATERTHAN OR EQUAL 9.50

MAXIMUM DATA VALUE 9.19
MINIMUM DATA VALUE -1.77
STRESSES IN MPa

Fig. 10 Minor principal stress contour plot for section x = 88.39 m.



MINOR PRINCIPAL STRESS CONTOURS X=82.29 M

LEGEND

SYMBOL	RANGE
-	LESS -5.00E-1
A	-5.00E-1 - 0.0
B	0.0 - 5.00E-1
C	5.00E-1 - 1.00
O	1.00 - 1.50
E	1.50 - 2.00
F	2.00 - 2.50
G	2.50 - 3.00
H	3.00 - 3.50
I	3.50 - 4.00
J	4.00 - 4.50
K	4.50 - 5.00
L	5.00 - 5.50
M	5.50 - 6.00
N	6.00 - 6.50
O	6.50 - 7.00
P	7.00 - 7.50
Q	7.50 - 8.00
R	8.00 - 8.50
S	8.50 - 9.00
T	9.00 - 9.50
+	GREATER OR EQUAL 9.50

MAXIMUM DATA VALUE 9.19
MINIMUM DATA VALUE -1.55E-1
STRESSES IN MPa

Fig. 11 Minor principal stress contour plot for section x = 82.29 m

As expected, mining of C-102-19 stope and C-102-21 stope on the lower mining block, and extracting of support pillars on the upper lever under existing far field stresses, results in the development of high compressive stress conditions (a maximum value of 25.6 MPa) around the lower portion of stopes C-102-19 and C-102-21. However, these stresses are not high enough to create zones of shear failure. Tensile stresses occur in stope roof and floor, and along the pillar wall. A maximum tension of 1.77 MPa occurs in the hangingwall or footwall of stope C-102-21 at the lower level.

The results can be summarized as follows:

- (a) Under existing stress conditions, the effect of excavating stopes C-102-19, C-102-21 and pillar T-102-19 below the sill pillar and extracting support pillars of the upper block on the overall stope/pillar stability will be nominal. The integrity of the sill pillars is not affected and only small tensile stresses were developed along the roof of stope C-102-21. The largest compressive stresses occur near stope corners with a magnitude of about 26.4 MPa . They are not sufficiently high to cause stability problems in terms of shear failure.
- (b) When all the upper level support pillars are extracted the stope span will be increased to approximately 274m. Tensile stress imposed to the roof and/or pillar walls of the large opening are relatively small; these tensile stresses are less than 1.0 MPa . However, the maximum tensile stress is approximately 1.77 MPa , and occurs at hangingwall or footwall at the lower level, as shown in Fig. 10. The tensile strength of carbonatite is estimated at $5 - 10 \text{ MPa}$ by laboratory testing; unless joints are unfavorably orientated, stope wall stability at the the lower level should not be a problem.

3.2 Potential Failure Areas

As mentioned in the previous reports [3,4,5], it is difficult to find a realistic failure criterion for a rock mass surrounding an underground excavation, since the stability of the rock in the immediate vicinity of underground openings is related to pre-existing discontinuities and fractures induced in the rock by blasting, and drilling processes, etc. Back analysis seems to be a rational approach and should be considered in any future study. At the moment, the mining of stope C-102-23 is almost completed. Visual observations indicate no instability around the mine opening.

No one criterion is capable of predicting potential ground failure for all types of rock. The Drucker/Prager yield criterion takes into account triaxial stress conditions but fails to consider any tensile failure. In recent years, Hoek and Brown's empirical failure criterion appears to be gaining popularity in rock mechanics applications. Although it

does not take into consideration intermediate principal stress, it does take into account rock mass quality and both shear and tensile modes of failure.

3.2.1 Drucker/Prager Yield Criterion

The Drucker/Prager yield criterion as adopted in the previous reports [3,4,5] for stope/pillar stability analyses was applied for this study. As an indicator for potential failure around stopes, the strength/stress ratio or the local factors of safety (LFS) in terms of the Drucker/Prager yield function have been calculated for the four sections under consideration, i.e., for the planes $x = 102.87\text{m}$, 95.25m , 88.39m and 82.29m .

The material constants used in this analysis were $C = 4 \text{ MPa}$ and $\phi = 40^\circ$, where C is the cohesive strength and ϕ the angle of internal friction. A value of $C = 4 \text{ MPa}$ used in shear failure analysis were considered to be reasonable and would provide conservative estimate of structural performance [5]. On this basis, the local factors of safety or the strength/stress ratio calculated for the pillars and stope walls appear to be more than adequate. The contour maps of LFS are shown in Figs. 12, 13, 14 and 15. The minimum LFS is 1.24. Therefore, no imminent shear failure is anticipated. If failure should occur, it would be localized tensile failure rather than shear failure.

3.2.2 Hoek and Brown's Empirical Failure Criterion

The Hoek and Brown's empirical failure criterion [7,8] is also applied.

Little information was available on the m and s values for the Niobec mine rocks. However, the $RQD's$ for the limestone, the intact and altered carbonatite are estimated as 90%, 95% and 90%, respectively. They are all representative of very good quality rock mass.

A series of analytic studies, using $m = 3.30$ and $s = 0.1111$ for both altered and intact carbonatite, were conducted. These values were also considered reasonable and would provide conservative estimates [4,5].

The strength/stress ratio maps, for the same sections described above, are shown in Figs. 16, 17, 18 and 19. Only small areas located at the roof, wall and floor of C-102-21 stope have strength/stress ratio less than 1.0 (Fig. 16).

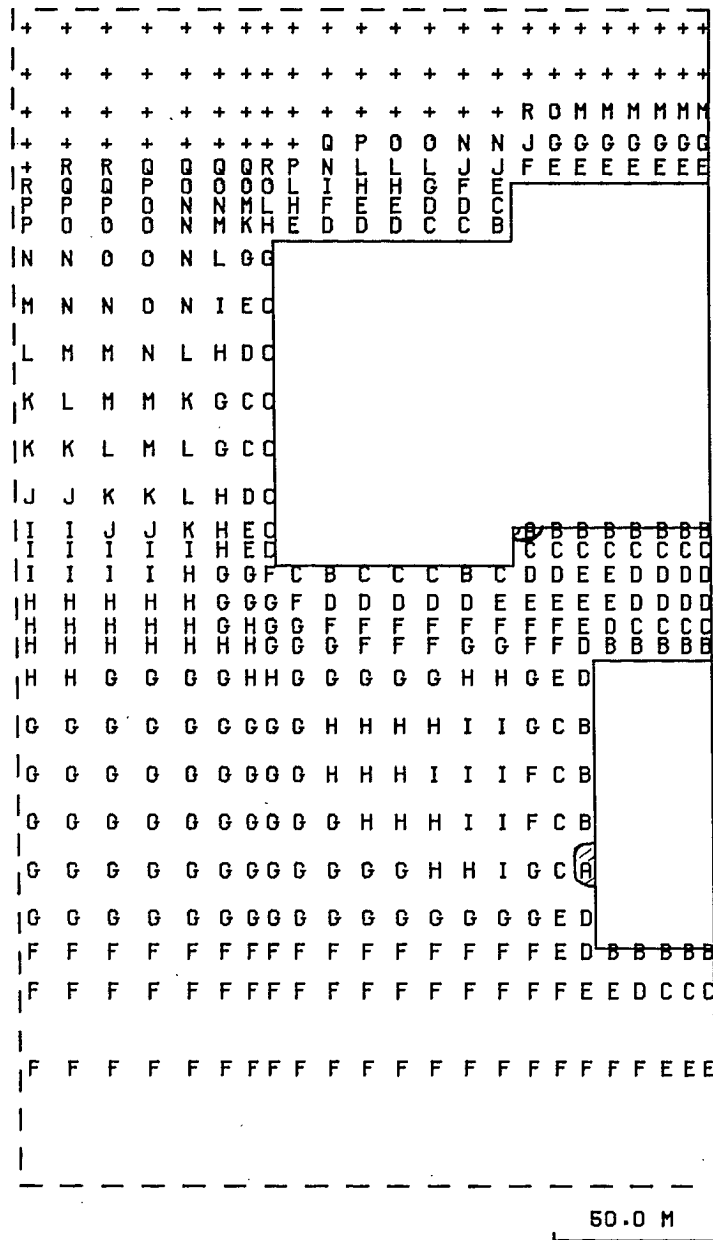
The strength/stress ratio or local factors of safety calculated for the pillars or stope walls based on the above assumptions, should be adequate against shear failure. However, Hoek & Brown's empirical failure criterion does not consider the orientation of joints. In a tensile zone, even when the strength/stress ratio is greater than one, tensile

failure is still possible depending on joint orientation. Therefore, localized failure could be anticipated.

4.0 CONCLUSIONS

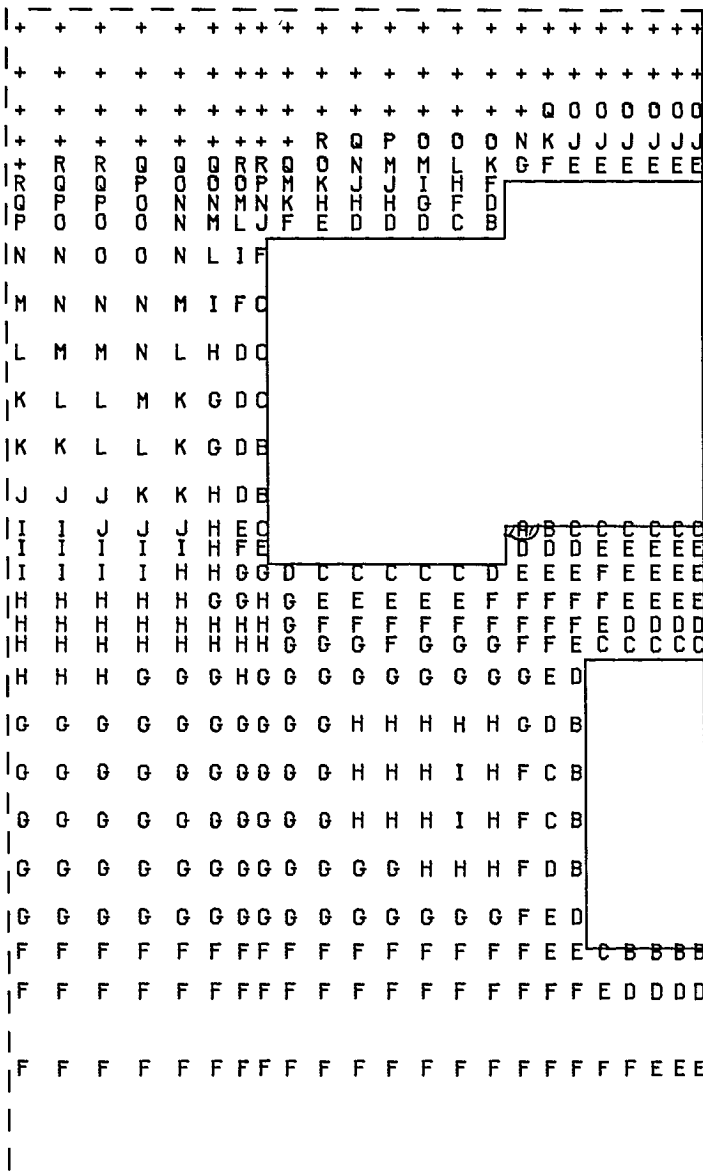
Following are the main conclusions of this study:

- (a) The effect of mining of C-102-19 and C-102-21 stopes in the lower block as well as extracting support pillars of the upper block on the overall stope/pillar ground stability conditions in the area under consideration, will be nominal.
- (b) As expected, the mining of C-102-21 and C-102-19 (mirror image of stope C-102-21) stopes on the lower level and the extracting of support pillars on the upper level will induce higher compressive stresses at the lower portion of the stopes. Compressive stress levels of about 26.4 MPa are developed near the stope wall; however, they are not sufficiently high to cause a ground stability problem.
- (c) Based on the Drucker/Prager yield criterion, as well as Hoek & Brown's empirical failure criterion, a series of stability analysis studies was carried out. The values of 4 MPa, 40° , 3.30, and 0.1111, for cohesive strength C , angle of internal friction ϕ , and empirical constants m and s , respectively, were used in the analyses. Results based on Drucker/Prager yielding analyses indicated no potential failure zones are developing around the stopes. However, Hoek & Brown's empirical failure analyses did show strength/stress ratio of less than 1 around stopes at the lower level; these failures occurred only in small areas and are considered to be localized and should not affect the overall structural stability. The material properties assumed in both analyses were considered conservative. Therefore, large shear failure is not anticipated. If failure should occur, it would be localized tension failure rather than shear failure.
- (e) Tensile stresses occur in stope roof walls and floor. Although these stresses are small (0 - 1.77 MPa) when compared with the tensile strength of carbonatite (5 - 10 MPa), localized tensile failure may develop if joints are oriented unfavorably with respect to tensile stresses. In other words, the structural stability of the stope walls will be greatly influenced by the presence of vertical or sub-vertical joints. Therefore, as mining progress, it should subject to continuous observations for stopes on both upper and lower levels.
- (f) As indicated in Figs. 10, and 11, tensile stresses may penetrate approximately 9m into the N-S walls of the large stope when all the support pillars are extracted and the stope C-102-21 (lower block). To delineate this potential fracture zone, it



LOCAL FACTOR OF SAFETY (DRUCKER/PRAGER) X=102.87 M.

Fig. 12 Local factor of safety contour plot ($C=4$ MPa, $\phi = 40^\circ$) for section $x = 102.87$ m.



LEGEND

SYMBOL	RANGE
-	LESS 1.00
A	1.00 - 1.50
B	1.50 - 2.00
C	2.00 - 2.50
D	2.50 - 3.00
E	3.00 - 3.50
F	3.50 - 4.00
G	4.00 - 4.50
H	4.50 - 5.00
I	5.00 - 5.50
J	5.50 - 6.00
K	6.00 - 6.50
L	6.50 - 7.00
M	7.00 - 7.50
N	7.50 - 8.00
O	8.00 - 8.50
P	8.50 - 9.00
Q	9.00 - 9.50
R	9.50 - 1.00E1
+	GREATER OR EQUAL 1.00E1

MAXIMUM DATA VALUE 1.00E1

MINIMUM DATA VALUE 1.49

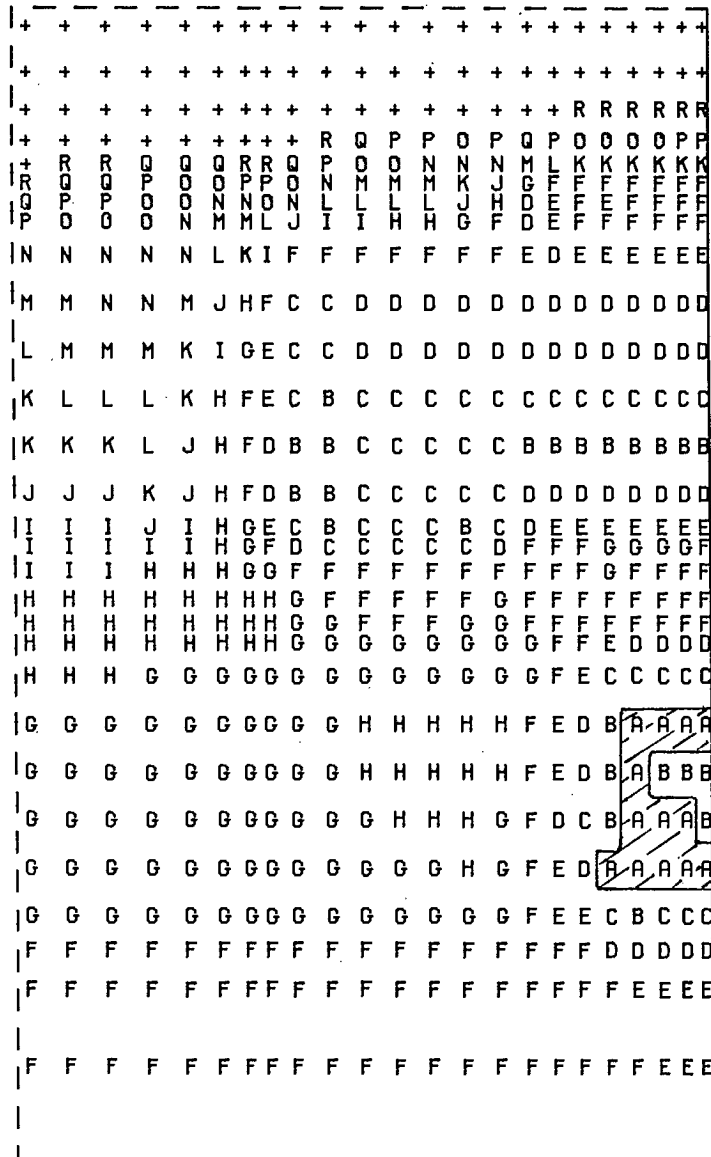
DRUCKER/PRAGER :

C = 4.0 MPa

PHI = 40.0 DEG.

LOCAL FACTOR OF SAFETY (DRUCKER/PRAGER) X=95.25 M.

Fig. 13 Local factor of safety contour plot ($C=4$ MPa, $\phi = 40^\circ$) for section $x = 95.27$ m.



LEGEND

SYMBOL	RANGE
-	LESS 1.00
A	1.00 - 1.50
B	1.50 - 2.00
C	2.00 - 2.50
D	2.50 - 3.00
E	3.00 - 3.50
F	3.50 - 4.00
G	4.00 - 4.50
H	4.50 - 5.00
I	5.00 - 5.50
J	5.50 - 6.00
K	6.00 - 6.50
L	6.50 - 7.00
M	7.00 - 7.50
N	7.50 - 8.00
O	8.00 - 8.50
P	8.50 - 9.00
Q	9.00 - 9.50
R	9.50 - 1.00E1
+	GREATER OR EQUAL 1.00E1

MAXIMUM DATA VALUE 1.00E1

MINIMUM DATA VALUE 1.13

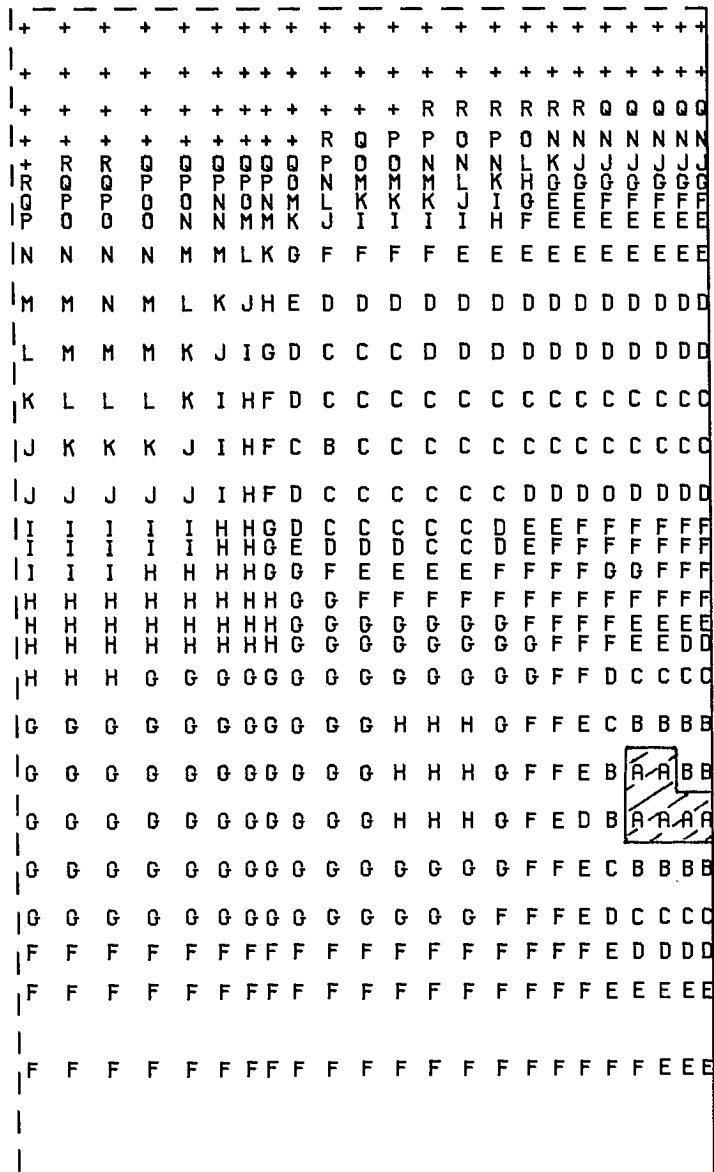
DRUCKER/PRAGER :

C = 4.0 MPa

PHI = 40.0 DEG.

LOCAL FACTOR OF SAFETY (DRUCKER/PRAGER) X=88.39 M.

Fig. 14 Local factor of safety contour plot ($C=4$ MPa, $\phi = 40^\circ$) for section $x = 88.39$ m.



LEGEND

SYMBOL	RANGE	
-	LESS	1.00
A	1.00	- 1.50
B	1.50	- 2.00
C	2.00	- 2.50
D	2.50	- 3.00
E	3.00	- 3.50
F	3.50	- 4.00
G	4.00	- 4.50
H	4.50	- 5.00
I	5.00	- 5.50
J	5.50	- 6.00
K	6.00	- 6.50
L	6.50	- 7.00
M	7.00	- 7.50
N	7.50	- 8.00
O	8.00	- 8.50
P	8.50	- 9.00
Q	9.00	- 9.50
R	9.50	- 1.00E1
+	GREATER OR EQUAL	1.00E1

MAXIMUM DATA VALUE 1.00E1

MINIMUM DATA VALUE 1.40

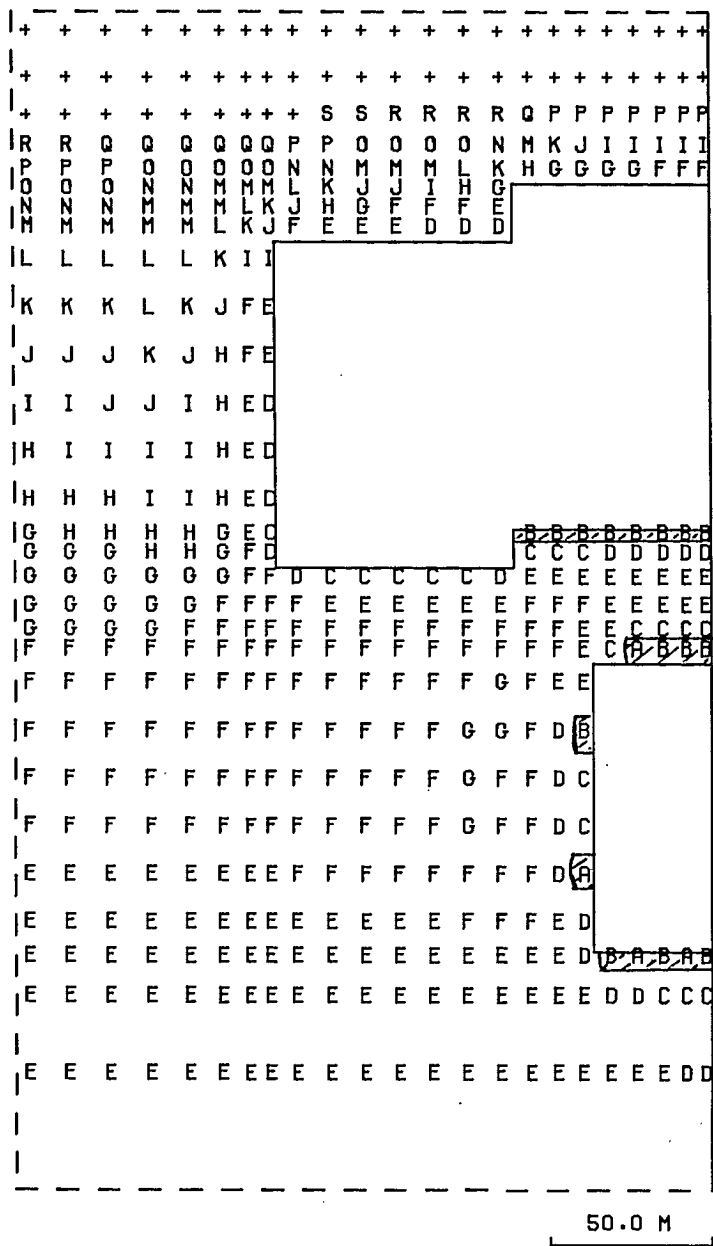
DRUCKER/PRAGER :

C = 4.0 MPa

PHI = 40.0 DEG.

LOCAL FACTOR OF SAFETY (DRUCKER/PRAGER) X=82.29 M.

Fig. 15 Local factor of safety contour plot ($C=4$ MPa, $\phi = 40^\circ$) for section $x = 82.29$ m.



HOEK & BROWN'S STRENGTH/STRESS RATIO X=102.87 M.

LEGEND

SYMBOL	RANGE
-	LESS 5.00E-1
R	5.00E-1 - 1.00
B	1.00 - 1.50
C	1.50 - 2.00
D	2.00 - 2.50
E	2.50 - 3.00
F	3.00 - 3.50
G	3.50 - 4.00
H	4.00 - 4.50
I	4.50 - 5.00
J	5.00 - 5.50
K	5.50 - 6.00
L	6.00 - 6.50
M	6.50 - 7.00
N	7.00 - 7.50
O	7.50 - 8.00
P	8.00 - 8.50
Q	8.50 - 9.00
R	9.00 - 9.50
S	9.50 - 1.00E1
+	GREATER OR EQUAL 1.00E1

MAXIMUM DATA VALUE 1.00E1

MINIMUM DATA VALUE 8.03E-1

HOEK/BROWN :

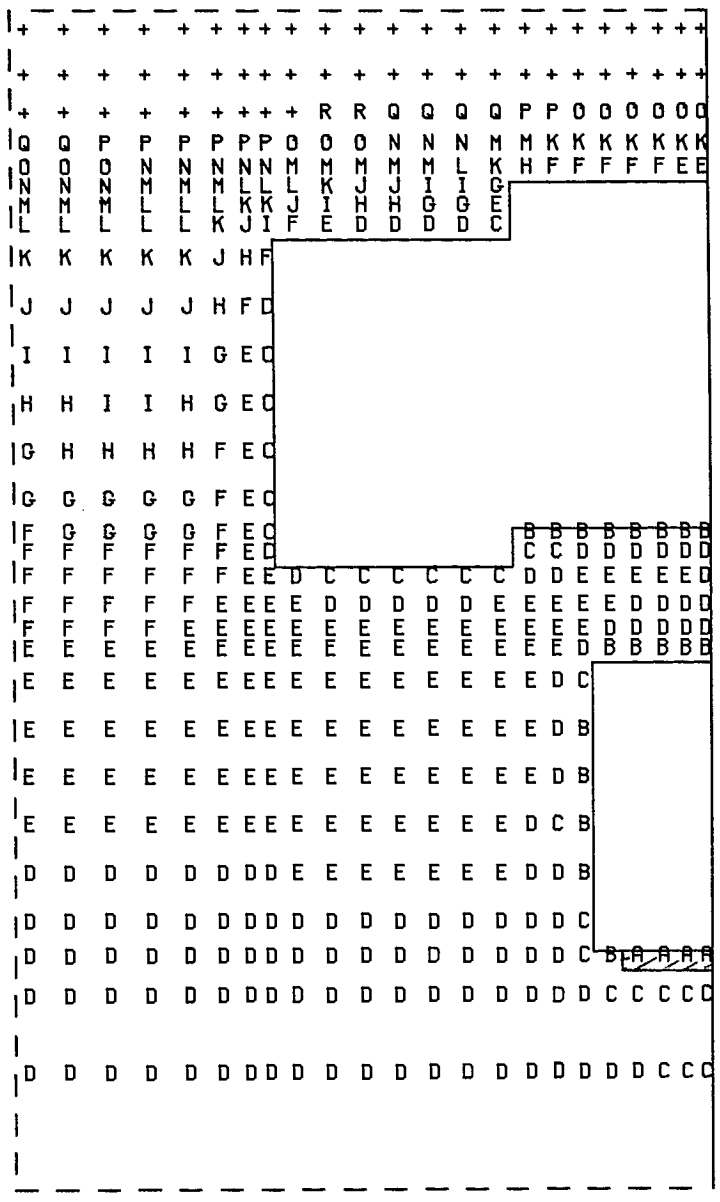
$$M = 3.3000$$

$$S = 0.1111$$

$$QU = 45.0 \text{ MPa}$$

Fig. 16 Strength/stress ratio - Hoek & Brown's empirical failure criterion ($m = 3.30$, $s = 0.1111$)

for section x = 102.87 m.



LEGEND

SYMBOL	RANGE	
-	LESS 1.00	
R	1.00	- 1.50
B	1.50	- 2.00
C	2.00	- 2.50
D	2.50	- 3.00
E	3.00	- 3.50
F	3.50	- 4.00
G	4.00	- 4.50
H	4.50	- 5.00
I	5.00	- 5.50
J	5.50	- 6.00
K	6.00	- 6.50
L	6.50	- 7.00
M	7.00	- 7.50
N	7.50	- 8.00
O	8.00	- 8.50
P	8.50	- 9.00
Q	9.00	- 9.50
R	9.50	- 1.00E1
+	GREATER OR EQUAL 1.00E1	

MAXIMUM DATA VALUE 1.00E1

MINIMUM DATA VALUE 1.42

HOEK/BROWN :

$M = 3.3000$

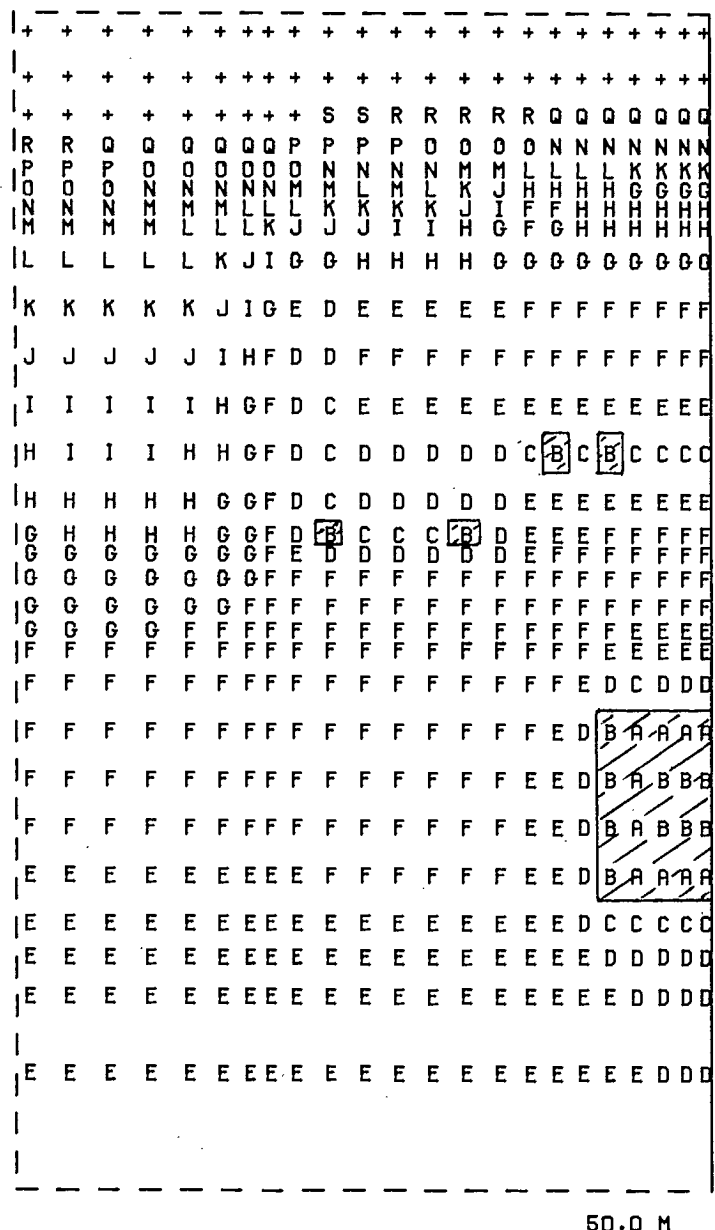
$S = 0.1111$

$Q_u = 45.0 \text{ MPa}$

HOEK & BROWN'S STRENGTH/STRESS RATIO X=95.25 M.

Fig. 17 Strength/stress ratio - Hoek & Brown's empirical failure criterion ($m = 3.30$, $s = 0.1111$)

for section x = 95.25 m.



HOEK & BROWN'S STRENGTH/STRESS RATIO X=88.39 M.

LEGEND

SYMBOL	RANGE	
-	LESS 5.00E-1	
A	5.00E-1	- 1.00
B	1.00	- 1.50
C	1.50	- 2.00
D	2.00	- 2.50
E	2.50	- 3.00
F	3.00	- 3.50
G	3.50	- 4.00
H	4.00	- 4.50
I	4.50	- 5.00
J	5.00	- 5.50
K	5.50	- 6.00
L	6.00	- 6.50
M	6.50	- 7.00
N	7.00	- 7.50
O	7.50	- 8.00
P	8.00	- 8.50
Q	8.50	- 9.00
R	9.00	- 9.50
S	9.50	- 1.00E1
+	GREATER OR EQUAL 1.00E1	

MAXIMUM DATA VALUE 1.00E1

MINIMUM DATA VALUE 5.00E-1

HOEK/BROWN :

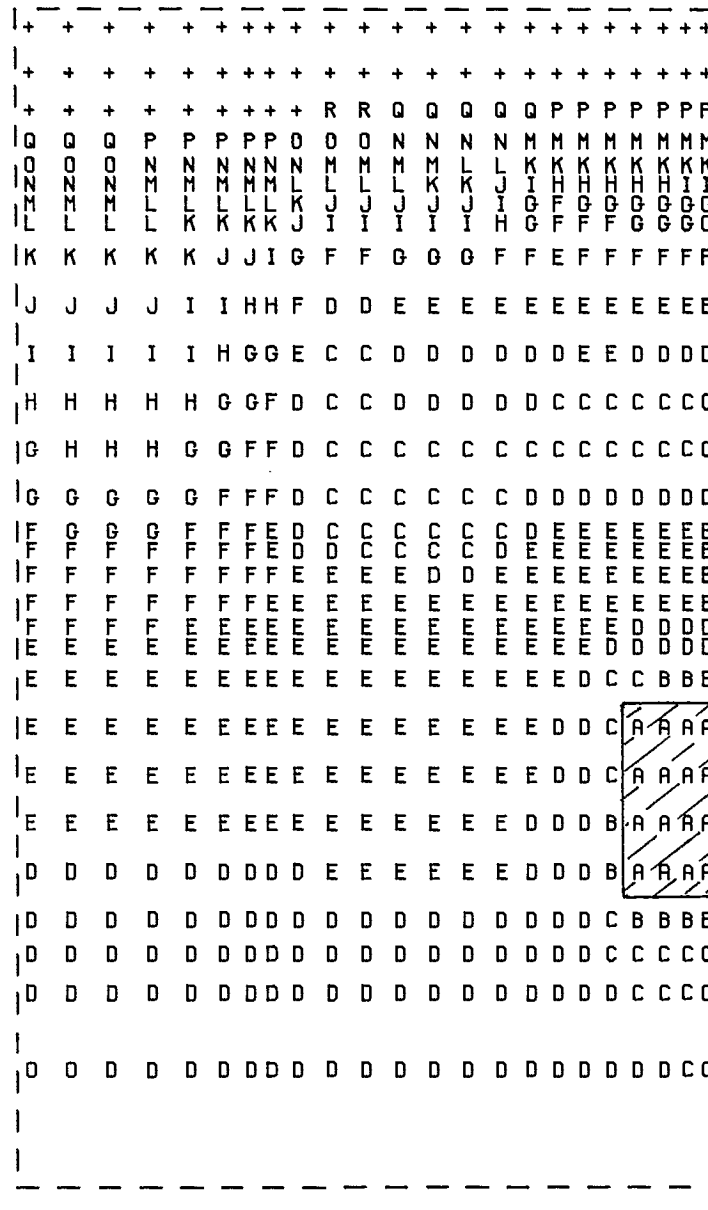
$M = 3.3000$

$S = 0.1111$

$QU = 45.0 \text{ MPa}$

Fig. 18 Strength/stress ratio - Hoek & Brown's empirical failure criterion ($m = 3.30$, $s = 0.1111$)

for section x = 88.39 m.



LEGEND

SYMBOL	RANGE	
-	LESS 1.00	
A	1.00	- 1.50
B	1.50	- 2.00
C	2.00	- 2.50
D	2.50	- 3.00
E	3.00	- 3.50
F	3.50	- 4.00
G	4.00	- 4.50
H	4.50	- 5.00
I	5.00	- 5.50
J	5.50	- 6.00
K	6.00	- 6.50
L	6.50	- 7.00
M	7.00	- 7.50
N	7.50	- 8.00
O	8.00	- 8.50
P	8.50	- 9.00
Q	9.00	- 9.50
R	9.50	- 1.00E1
+	GREATER OR EQUAL 1.00E1	

MAXIMUM DATA VALUE 1.00E1

MINIMUM DATA VALUE 1.09

HOEK/BROWN :

$m = 3.3000$

$s = 0.1111$

$q_u = 45.0 \text{ MPa}$

HOEK & BROWN'S STRENGTH/STRESS RATIO X=82.29 M.

Fig. 19 Strength/stress ratio - Hoek & Brown's empirical failure criterion ($m = 3.30$, $s = 0.1111$)

for section x = 82.29 m.

would be useful if multi-wire extensometers were installed in the N-S walls of the large stope on the upper level and stope below the sill pillar before they were fully developed. This has been suggested in a previous study [4]. In addition, a well-designed visual inspection program should also be useful. This information could be used for back analysis and verification of the finite element model and increase confidence in the future use of modelling.

5.0 ACKNOWLEDGEMENTS

The excellent cooperation received from the Niobec Mine Ltd., and Centre de Recherches Minérales, Quebec, is acknowledged. The authors wish to thank the management of Mining Research Laboratories of CANMET for their encouragement and support in this project. The authors also wish to thank M. Bétournay for his function as a liaison officer between the Canadian Mine Technology Laboratory and the Niobec Mine.

6.0 REFERENCES

1. Arjang, B.; "Field Stress Determinations at the Niobec Mine, Chicoutimi, Quebec"; Division Report MRL 87-15 (TR); Mining Research Laboratories, CANMET, Energy, Mines and Resources Canada; Dec., 1986.
2. Yu, Y.S., S. Vongpaisal, Toews, N.A. and Wong, A.S.; "A Preliminary Stability Assessment of C-102-23 Stope of the Niobec Mine Under Gravitational Loading"; Division Report M&ET/MRL 86-97 (TR); Mining Research Laboratories, CANMET, Energy, Mines and Resources Canada; July, 1986.
3. Yu, Y.S., Vongpaisal, S., Wong, A.S. and Toews, N.A.; "Stability Assessment of C-102-23 Stope of the Niobec Mine Under Tectonic Stresses - Part II"; Division Report M&ET/MRL 86-145 (TR); Mining Research Laboratories, CANMET, Energy, Mines and Resources Canada; Dec., 1986.
4. Yu, Y.S., Wong, A.S., Vongpaisal, S. and Toews, N.A.; "Stability Assessment of S-L-102-17 Sill Pillar of the Niobec Mine, Chicoutimi, Quebec - Part III"; Division Report MRL 87-96 (TR); Mining Research Laboratories, CANMET, Energy, Mines and Resources Canada; Dec., 1986.
5. Yu, Y.S., M.C. Bétournay, G.E. Larocque and S. Thivierge; Pillar and Stope Stability Assessment of the Niobec Mine Using the Three-Dimensional Finite Element Techniques; Prepared for presentation at the 15th Canadian Rock Mechanics Symposium, October 3-4, 1988, Toronto, Ontario; Division Report MRL

- 88-68 (OP,J); Mining Research Laboratories, CANMET, Energy, Mines and Resources Canada; July, 1988.
6. Labrie, D.; "Étude de Stabilité à la Mine Niobec"; Project STM-526, Centre de Recherches Minérales, Quebec; October, 1986.
 7. Bétournay, M.C., Gorski, B. and Situm, M.; "Tétrauville Limestone of the Niobec Surface Crown Pillars: Comparison of Strength and Deformation Properties from Various Tests"; Division Report M&ET/MRL 86-144 (TR); Mining Research Laboratories, CANMET, Energy, Mines and Resources Canada; Dec., 1986.
 8. Hoek, E., and Brown, E.T.; "Underground Excavations in Rock"; Stephen Austin and Sons Ltd., Hertfort, England; 1980.
 9. Elsayed Armed Eissa; "Stress Analysis of Underground Excavations in Isotropic and Stratified Rock Using the Boundary Element Method"; Ph.D Thesis, Imperial College of Science and Technology, 1980.

